New sequence data enable modelling of the fungal alternative oxidase and explain an absence of regulation by pyruvate

Tim Joseph-Horne[a], Joanna Babij[b], Paul M. Wood[a], Derek Hollomon[b], Richard B. Sessions[a],*

[a]Department of Biochemistry, School of Medical Sciences, University of Bristol, University Walk, Bristol BS8 1TD, UK
[b]IACR-Long Ashton Research Station, Department of Agricultural Sciences, University of Bristol, Long Ashton, Bristol BS41 9AF, UK

Abstract Respiratory rates involving the alternative oxidase (AO) were studied in mitochondria from *Tapesia acuformis*. There was no evidence for regulation by pyruvate, in contrast with plant AO. The site of interaction of pyruvate with the plant AO is a conserved cysteine. The primary sequence was obtained for AO from *Magnaporthe grisea* and compared with four published sequences for fungal AO. In all cases this cysteine was absent. Sequence data were obtained for the C-terminal domain of a further five fungal AOs. In this region the fungal sequences were all consistent with a four-helix, di-iron binding structure as in the ferritin-fold family. A molecular model of this domain was deduced from the structure of Δ-9 desaturase. This is in general agreement with that developed for plant AOs, despite very low sequence identity between the two kingdoms. Further modelling indicated an appropriate active site for binding of ubiquinol, required in the AO redox reaction. © 2000 Federation of European Biochemical Societies. Published by Elsevier Science B.V. All rights reserved.

Key words: Fungal alternative oxidase; Mitochondrial electron transport; Pyruvate regulation; Molecular modelling; *Magnaporthe grisea*

1. Introduction

Whilst most fungi retain a 'core' mitochondrial electron transfer chain, similar to that utilised by mammalian mitochondria, various additional redox components have been identified providing fungi with a highly branched electron transfer chain [1]. A particular branch point within the fungal pathway enables partitioning of electrons away from the 'core' cytochrome pathway to an alternative oxidase (AO), thereby by-passing complex III and complex IV [2–4]. Until recently, fungal AO was considered to be a functional analogue of that from plants. However, recent research questions the validity of this assumption as many of the functional and regulatory processes of fungal AO appear distinct from those associated with plant AO [1]. Perhaps unsurprisingly, plant AO is regulated by α-keto acids, especially pyruvate, which bind to the plant AO forming a thiohemiacetal [5]. Site-directed mutagenesis of a highly conserved cysteine residue (Cys-78) in *Arabidopsis thaliana* abolishes this regulation [6].

AO provides plant cells with the capacity to uncouple electron transfer from proton translocation. Such a function enables continued cycling of trichloroacetic acid cycle intermediates during developmental periods or stress conditions, such as cold, wounding, flowering, or when the energy requirement of the cell is low [7–9]. However, uncoupling electron transfer completely from proton translocation within pathogenic fungi would be anticipated to be highly detrimental to cell survival as nutrient availability is likely to be low, especially during the initial stages of pathogenesis when the fungi is utilising stored nutrients. Significantly, and unlike plant AO, activity of fungal AO is raised in response to a decrease in the matrix ATP:ADP ratio [7,10,11] indicating that fungi may use AO in a role unlike that of plant cells. Supporting this differing role is the observation that inhibition of an active fungal AO prevents the establishment and maintenance of mitochondrial membrane potential ($\Delta\psi$), thereby decreasing oxidative phosphorylation [4]. Furthermore, the magnitude of decrease for either $\Delta\psi$ or ATP has been reported to be equivalent to that observed with inhibitors of the core electron transport chain such as antimycin A or cyanide [4].

Prior to this project, sequence information for fungal AO was confined to five species: *Aspergillus niger* [12], *Candida albicans* [13], *Hansenula anomala* [14], *Magnaporthe grisea* [15] and *Neurospora crassa* [16]. This paper reports data for a further six species or strains, which are all plant pathogens: *Botrytis cinerea* (grey mould), *Gaeumannomyces graminis* var. *tritici* (take-all), *Magnaporthe grisea* (rice blast), *Rhizoctonia solani* (black scurf of potato*), Septoria nodorum* (leaf and glume blotch) and *Tapesia acuformis* (eyespot). The complete sequence has been obtained for a *M. grisea* strain, which differs slightly from one obtained recently [15]. The other sequences are complete for the C-terminal iron-binding domain, for which a detailed model is presented and compared with those derived for plant AO [17,18]. Discussion of the N-terminal domain primarily concerns a conserved cysteine in the plant AO, which has been shown by mutagenesis to be obligatory for pyruvate regulation.

2. Materials and methods

2.1. Materials

All chemicals, unless otherwise stated, were purchased from Sigma, Poole, UK, and were of the highest purity. Stock solutions of antimycin A (19 mM based on an average formula weight 527.6 as a mixture of antimycin A_1, A_2, A_3 and A_4), propyl gallate (500 mM), rotenone (20 mM) and potassium cyanide (500 mM).

2.2. Strains and plasmids

G. graminis strain T7 was a gift from Dr Paul Bowyer, IACR-Long Ashton Research Station, UK. *B. cinerea* and *R. solani* were supplied by Dr Hideo Ishii, NIAES, Japan, and *T. acuformis* and *S. nodorum*,

*Corresponding author. Fax: (44)-117-9288274.
E-mail: r.sessions@bristol.ac.uk

were isolated at IACR-Long Ashton Research Station, UK. All fungal cultures were maintained at 18°C on potato dextrose media (Oxoid) containing agar (2% w/v) except *G. graminis* which was maintained on Czapek Dox Agar (Oxoid) supplemented with D-biotin (0.2 μg/ml) and thiamine (0.2 μg/ml). *Escherichia coli* host strain was DH5α, and the cloning plasmid was pGEM-T vector (Promega, UK).

2.3. Pyruvate regulation of fungal AO

Mitochondria were isolated from *T. acuformis* according to the method described by Tamura et al. [19]. Mycelia were collected by centrifugation (4200×*g*) and washed three times in isolation buffer (30 ml; KH_2PO_4 (0.1 mM), K_2HPO_4 (0.1 mM) (pH 7.4), disodium EDTA (1 mM) and reduced glutathione (1 mM)). Pelleted mycelia were homogenised with glass beads, followed by centrifugation at 6000×*g*, for 10 min at 4°C to remove beads, whole cells and large cellular particulates. The mitochondrial fraction was obtained by centrifugation at 20 000×*g* for 25 min at 4°C and the resultant mitochondrial pellet resuspended in isolation buffer (1 ml) containing 20% glycerol. A 10 μl aliquot of this suspension was removed for protein concentration estimation and the remainder either used immediately or frozen in liquid nitrogen and stored at −80°C. These preparations remained active for at least 6 months, but were typically used fresh or within 1 week of isolation. Mitochondrial inner membrane integrity was assessed from the capacity to generate $\Delta\psi$ upon addition of respiratory substrates according to the method described previously [4].

2.4. Measurement Of oxygen consumption in isolated mitochondria

Mitochondrial oxygen consumption was measured at 18°C with a Clark-type oxygen electrode (Oxygraph DW1, Hansatech, UK) in phosphate buffer (1 ml; 50 mM potassium phosphate (pH 7.4) sucrose (0.25 mM), $MgCl_2$ (5 mM), KCl (10 mM) and bovine serum albumin (BSA; 1 g l^{-1})). Pyruvate and inhibitors were added at the concentrations indicated and oxygen consumption recorded over 20 min. Rates of oxygen consumption are expressed as μM O_2 min^{-1} mg $protein^{-1}$ or as percentages of the control rate. Oxygraph calibration was conducted according to the manufacturer's protocol with the oxygen saturation point in 1 ml dH_2O at 18°C being approximately 288 nmol.

2.5. Protein estimation

Protein concentrations were measured using the BCA protein assay reagent system (Pierce, Chester, UK) adapted for a 96-well microtitre plate assay. Absorbance values (560 nm) were converted to mg protein ml^{-1} with reference to a BSA standard curve.

2.6. Genomic DNA manipulation

Genomic DNA was isolated from fresh mycelia of *M. grisea* (kindly supplied by Dr M.-C. Grosjean, Aventis Crop Science, Lyon, France) and from *G. graminis*, *S. nodorum*, *T. acuformis* and *R. solani* according to the standard protocol [20]. Full length and partial AO sequences were obtained by polymerase chain reaction (PCR) following standard amplification protocols employing degenerate primers designed from conserved regions identified from published fungal AO nucleotide sequences. Amplification products were cloned into pGEM-T vector (Novagen) prior to sequencing by the dideoxy chain-termination method of Sanger et al. [21] using the Sequenase kit, version 2.0 (United States Biochemical). All clones were sequenced as sense and anti-sense strands.

2.7. Molecular modelling

The structure-based sequence alignment of representative members of the SCOP database [22] ferritin-like fold family was obtained by superimposing structurally conserved regions of the 4-helix bundles of bacterioferritin (1bcf), rubrerythrin (1ryt), ribonucleotide reductase (1xik) and methane mono-oxygenase (1mhy) onto Δ-9 desaturase (1afr). The alignment was generated from this set of superimposed structures by inspection and is shown as the second group of sequences in Fig. 2.

In general, multiple sequence alignments were carried out using Pileup and pairwise alignments using Bestfit (GCG). The homology model of the C-terminal domain of *M. grisea* (*M. grisea*-C) was built on the Δ-9 desaturase protein (1afr) according to the alignment in Fig. 2, using standard methods [23]. A substrate complex was generated by constraining an oxygen molecule to lie between the two Fe ions to give a μ-1,2 peroxo complex, then ubiquinol was docked into the

active site such that the aromatic ring of the ligand lay over the di-iron centre. A model of the putative dimer was generated by juxtaposing helix-3 of one monomer with helix-3 of a second monomer in an antiparallel alignment. These models were energy minimised according to the following protocol: the models were surrounded by a 5 Å layer of water, protein backbone atoms were constrained to their initial positions by a harmonic potential and this restraining force was reduced from 100 to 0.5 kcal/Å during 2000 cycles of conjugate gradient minimisation. The geometric quality of the models was assessed using Procheck.

Sequence database searching was carried out using GCG at the UK HGMP Resource Centre. Structure prediction was carried out using the Predict-Protein suite of software available on the EMBL web server (http://www.embl-heidelberg.de) and the accompanying meta-server.

3. Results

3.1. Pyruvate regulation of T. acuformis AO

NADH driven oxygen consumption by mitochondria isolated from *T. acuformis* was assessed with a Clark-type oxygen electrode. Oxygen consumption driven by electrons supplied by succinate was lower (8.9 μM O_2 min^{-1} mg $protein^{-1}$) than that obtained with NADH (53.1 μM O_2 min^{-1} mg $protein^{-1}$) and, therefore, NADH was selected as the respiratory substrate. NADH driven oxygen consumption was only weakly sensitive to rotenone (34% decrease in oxygen consumption with 200 μM rotenone) indicating that *T. acuformis* mitochondria may utilise rotenone insensitive external NADH dehydrogenase(s) to introduce electrons from cytosolic NADH into the electron transport chain. Mitochondrial respiration was sensitive to both antimycin A (40 μM) and cyanide (1 mM) which inhibited oxygen consumption by 66 and 74%, respectively. In addition, these mitochondria were also sensitive to the AO inhibitor, propyl gallate (1 mM) which decreased oxygen consumption by 62%. However, maximal inhibition levels were not achieved unless either a complex III or IV inhibitor together with propyl gallate were employed. Thus, antimycin A (40 μM)+propyl gallate (1 mM) or cyanide (1 mM)+propyl gallate (1 mM) decreased oxygen consumption by 96 and 94%, respectively. Such data indicated that both core and AO pathways are present, and active, within mitochondria isolated from this fungus.

Two approaches were adopted to assess activity regulation of *T. acuformis* AO by pyruvate. The first sought evidence for
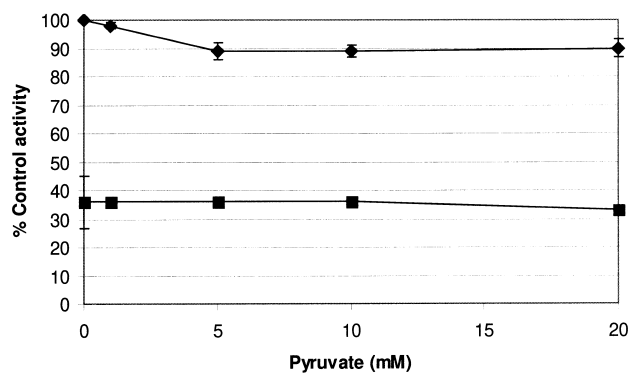

Fig. 1. Evaluation of pyruvate regulation of *T. acuformis* AO activity. ◆, pyruvate added to mitochondria in the absence of inhibitors; ■, pyruvate added to mitochondria pre-treated with cyanide (1 mM). Control activity was determined from isolated mitochondria utilising NADH (300 μM) as a respiratory substrate and in the presence of ADP (300 μM). All assays were conducted in triplicate.

```
AOX_ASPNG  [133] GTRGQVQNDRAEVLTRFIFLESV.AGVPGMVGGMLRHLRSLRRMKRDNGWIETLLEEAYNERMHLLTFLKLAEPGWFM
AOX_NEUCR  [142] ATSADKPLTEAQWLVRFIFLESI.AGVPGMVAAFIRHLHSLRLLKRDNGWIETLLEESYNERMHLLTFMKMCEPGLLM
AOX_HANAN  [123] GTRYE..MTEEKWLTRCIFLESV.AGVPGMVAAFIRHLHSLRLLKRDKAWIETLLDEAYNERMHLLTFIKIGNPSWFT
AF031229   [161] GTRWE..MTEEKWMTRCIFLESI.AGVPGSVAGFVRHLHSLRMLTRDKAWIETLHDEAYNERMHLLIFMNIKQPGYLE
RS         [Und] ~~~...~~~~~~~~~~~~~~~~~~~~~~~~~~~~~~~~~~~~~~~~~~~~~EAYNERMHLLTFLKMCEPGPWFL
T7         [Und] ~~~...~~~~~~~~~~~~~~~~~~~~~~~~~~~~~~~~~~~~~~~~~~~~~EAYNERMHLLTFLKMCEPGPWFL
TA         [Und] ~~~...~~~~~~~~~~~~~~~~~~~~~~~~~~~~~~~~~~~~~~~~~~~~~EAYNERMHLLTFLKMAEPGWFM
SN         [Und] ~~~...~~~~~~~~~~~~~~~~~~~~~~~~~~~~~~~~~~~~~~~~~~~~~EAYNERMHLLVFLKMQEPGPFM
BOT        [Und] ~~~...~~~~~~~~~~~~~~~~~AGIWRHLRSSRGLKRDNGWCIETLLEEAYNERMHLLTFLKMYEPGIFM
MG         [135] SIVGAKPLTEAQWLSRFIFLESI.AGVPGMVAGMLRHLHSLRRLKRDNGWIETLLEEAYNERMHLLTFLKMCEPGWLM
                                                                        helix 1              helix 2

STAD_RICCO [117] ERAKEIPDDYFVVLVGDMITEEA.LPTYQTMLNT.LDGVRDETGASPTSWAIWTRAWTAEENRHGDLLNKYLYLSGRV
BFR_ECOLI  [  0]    MKGDTKVINYLNKLLGNELV.AINQYFLHARM.......FKNWGLKRLNDVEYHESIDEMKHADRYIERILFLEGL
RUBY_DESVH [  0]  MKSLKGSRTEKNILTAFAGESQARNRYNYFGGQ.......AKKDGFVQISDIFAETADQEREHAKRLFKFLEGGDLE
RIR2_COLI  [ 33] ALPEHEKHIFISNLKYQTLLDSIQGRSPNVALLP.........LISIPELETWVETWAFSETIHSRSYTHIIRNIVND
MEMA_METTR [ 88] KVHPRWGETMKVISNFLEVGEYNAIAASAMLWDS.AT..........AAEQKNGYLAQVLDEIRHTHQCAFINHYYSKH

AOX_ASPNG  RLM.................................VLGAQGVFFNGFFLS..YLMSP.RICHRFVG.YLEEE.AV
AOX_NEUCR  KTL.................................ILGAQGVFFNAMFLS..YLISP.KITHRFVG.YLEEE.AV
AOX_HANAN  RFI.................................IYMGQGVFANLFFLV..YLIKP.RYCHRFVG.YLEEE.AV
AF031229   RSI.................................IYIGQGVFTNIFFLV..YLMNP.RYCHRFVG.YLEEE.AV
RS         RGL.................................VLGAQGVFFNGFFLT..YLVSP.KTCHRFVG.YLEEE.AV
T7         KML.................................ILGAQGLYFNALFVA..YLISP.KICHRFVG.YLEEE.AV
TA         KFM.................................ILGAQGVFFNSMFLS..YLISP.KTCHRFVG.YLEEE.AV
SN         RFM.................................VLAAQGVWCNAMFFA..YLISP.RIVHRLVG.YLEEE.AV
BOT        RTM.................................ILGAQGVFFNSFLLC..YLFYP.RTCHRFVG.YLEEE.AV
MG         KIL.................................IIGAQGVYFNAMFVA..YLISP.KICHRFVG.YLEEE.AV

STAD_RICCO DMR............................QIEKTIQYLIGSGMDPRTENSP.YLGFIYTS.FQERA.TF
BFR_ECOLI  PNL............................QDLGKLNIGEDV.EEMLRSDL.ALELD.GA
RUBY_DESVH IVA............................AFPAGIIADT.HANLIASA.AGEHH.EY
RIR2_COLI  PSVVFDDIVTNEQIQKRAEGISSYYDELIEMTSYWHLLGEGTHTVNGKTVTVSLRELKKKLYLCLMSVN.ALEAI.RF
MEMA_METTR YHDPAGHNDARRTRAIGPLWKGMKRVFADGF......................ISGDAVECSVNLQLVGEACFTN
                        hydrophobic linker                                    helix 3

AOX_ASPNG  .ITYTRAIKEIEAGSLPAW..EKTEAPEIAVQYWKMPEGQRSMKDLLLYVRADEAKHREVNHTLGNLNQAIDPNP [ 31]
AOX_NEUCR  .HTYTRCIREIEEGHLPKWSDEKFEIPEMAVRYWRMPEGKRTMKDLIHYIRADEAVHRGVNHTLSNLDQKEDPNP [ 31]
AOX_HANAN  .STYTHLIKDIDSKRLPKF..DDVNLPEISWLYWTDLNEKSTFRDLIQRIRADESKHREVNHTLANLEQKKDRNP [ 34]
AF031229   .RTYTHLIDELDDPNKLPDF.QKLPIPNIAVQYWPELTPESSFKDLILRIRADEAKHREINHTFANLEQWQDRNP [ 32]
RS         .H~~~~~~~~~~~~~~~~~~~~~~~~~~~~~~~~~~~~~~~~~~~~~~~~~~ [Und]
T7         .HTY~~~~~~~~~~~~~~~~~~~~~~~~~~~~~~~~~~~~~~~~~~~~~~~ [Und]
TA         .HTY~~~~~~~~~~~~~~~~~~~~~~~~~~~~~~~~~~~~~~~~~~~~~~~ [Und]
SN         .HTY~~~~~~~~~~~~~~~~~~~~~~~~~~~~~~~~~~~~~~~~~~~~~~~ [Und]
BOT        .LTYTLSIQDLENGHLPKWADPDFKAPDLAVEHWRMPEGYRSMRDLLYYILADEAKHPEVNHTLGNLKPDEDPNP [ 17]
MG         .HTFTRSIEELERGDLPKWSDPKFQVPEIAVSYWGMPEGHRTMRDLLLYIRADEANHRGVHHTLGNLNQVEDPNP [ 53]

STAD_RICCO .ISHGNTARQAK.......................EHGDIKLAQICGTIAADEKHETAYTKIVEKLFEIDPDG [113]
BFR_ECOLI  .KNLREAIGYAD.......................SVHDYVSRDMMIEILRDEEGHIDWLETEDLIQKMGLQN [ 10]
RUBY_DESVH TEMYPSFARIAR.......................EEGYEEIARVFASIAVAEEFHEKRFLDFARNIKEGRVFL [ 42]
RIR2_COLI  .YVSFACSFAFA.......................ERELMEGNAKIIRLIARDEALHLTGTQHMLNLLRSGADDP [116]
MEMA_METTR .PLIVAVTEWAS.......................ANGDEITPTVFLSVETDELRHMANGYQTVVSIANDPASA [261]
              helix 3                              helix 4
```
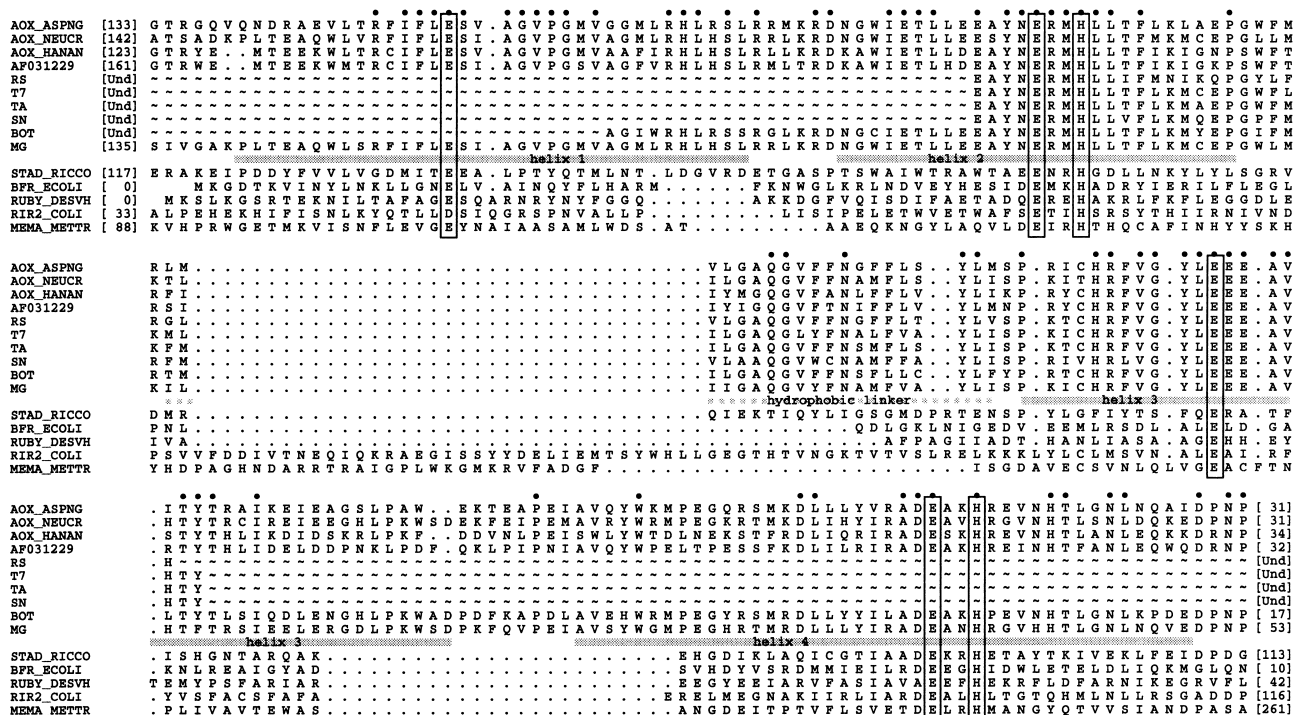
Fig. 2. Sequence alignment of the 4-helix bundle region within the C-terminal domain. The upper group is a pileup of all fungal AO sequences. The lower group is a structure-based alignment of members of the ferritin-like fold family. The upper and lower groups are aligned via the *M. grisea* and Δ-9 desaturase sequences. The numbers in square brackets indicate the number of residues which are present before or after the displayed sequence, Und indicates undetermined. Sequence keys are: AO_ASPNG, *A. niger*; AO_NEUCR, *N. crassa*; AO_HANAN, *H. anomala*; AF031229, *C. albicans*; RS, *R. solani*; T7, *G. graminis*; TA, *T. acuformis*; SN, *S. nodorum*; BOT, *B. cinerea*; MG, *M. grisea*; STAD_RICCO, Δ-9 desaturase from *Ricinus communis*; BFR_ECOLI, bacterioferritin from *E. coli*; RUBY_DESVH, rubrereythrin from *Desulfovibrio vulgaris*; RIR2_COLI, ribonucleotide reductase from *Escherichia coli*; MEMA_METTR, methane mono-oxygenase from *Methylosinus trichosporium*. The boxed residues are actual metal ligands (lower group) and proposed metal ligands (upper group). Conserved residues in fungal AOs are indicated by a dot above the position.

a pyruvate induced increase in respiratory rate within a fully functional electron transfer chain whilst the second monitored AO activity following the addition of pyruvate to mitochondria inhibited with cyanide (1 mM) or antimycin A (40 μM: data not shown) (Fig. 1). Whereas rates of NADH driven oxygen consumption in isolated plant mitochondria, or submitochondrial particles, are raised following pyruvate addition [24], no significant increase in the rate of oxygen consumption was observed for *T. acuformis* mitochondria following the addition of 1, 5, 10 or 20 mM pyruvate (Fig. 1). In a separate assay, mitochondria were pre-treated with cyanide (1 mM) to ensure that all respiration involved AO. Under such conditions, pyruvate had no effect on the rate of oxygen consumption (Fig. 1). These data strongly imply an absence of pyruvate regulation for *T. acuformis* AO.

3.2. Molecular analysis and modelling of fungal AO

3.2.1. Isolation of full length and partial sequences of fungal AO.
Clones obtained from PCR amplification of *M. grisea* genomic DNA were translated and the primary amino acid sequence compared with all other fungal AO sequences (Fig. 2). The gene was predicted to encode a protein of 377 residues with a molecular weight of 42.73 kDa, which is consistent with all other fungal AO examined to date [12–16]. The primary amino acid sequence is also closely similar to an AO recently obtained from a *M. grisea* strain [15], differing in four conservative amino acid changes (S120G, G139A, G160A and F253Y). Partial sequences from the following fungi were also

obtained by PCR; *G. graminis* (T7), *S. nodorum*, *T. acuformis*, *B. cinerea* and *R. solani*. These clones were also sequenced and identified as encoding for AO by comparison with published AO sequences. All clones retained high amino acid identity with other fungal AO, and contained the conserved residue motifs associated with all di-iron carboxylates (Fig. 2).

3.2.2. Attempts to model the N-terminal domain of M. grisea.
The N-terminal sequence of *M. grisea* was analysed in the hope of modelling the structure of this domain to provide a molecular insight into regulatory features of fungal AO. In the absence of crystallographic data it was hoped that this region might contain homology to better characterised proteins, thus providing potential templates for subsequent modelling. Unfortunately, no hits were found using Blast on the sequence database of known protein structures (nrl3d). The only significant hits found on searching the SwissProt database were other AOs. Secondary structure prediction using the Jpred consensus method gave no strong indication of secondary structure. Likewise the threading method Sam-t98 gave no consensus fold prediction. The Topits method behaved similarly and gave a low Zali score of 2.17 for the best hit. Consequently the only information we can glean from the N-terminal domain sequences comes from sequence alignment (Fig. 3).

3.2.3. Modelling the C-terminal domain of M. grisea.
The structure-based sequence alignment, shown as the lower set of five sequences in Fig. 2, is notable for the lack of conservation of amino acids. Sequence identities were calculated between

```
MG                             MLVHQVN..TKLCSAKQFT.HLAKVVTPALSYQASSVYSANLPRLAASPRLFSTTSSAQLRDFFPVKETEHIRQ...
AOX_NEUCR                      MNTPKVNILHAPGQAAQLSRALIST.CHTRPLLLAGSRVATSLHPTQTNLSSPSPRNFSTTSVTRLKDFFPAKETAYIRQ...
AF031229       MIGLSTYRNLPTLLTTTTVISTALRSKQLLRFTTTTSTKSRSSSTAATTVGNSNPKSPIDEDNLEKPGTIPTKHKPFNIQTE.VYNKAGIEANDDDKFL
AOX_HANAN                      MIKTYQYRSILNSRNVGIRFLKTLSPSPHSKD........PNSKSIFDIGTKLIVNPPPQMA..DNQYV
AOX_ASPNG                      MNSLTATAPIRAAIPKSYMHIATRNYSGVIAMSGLRCSGSLVANR..HQTAGKRFISTTPKSQIKEFFPPPTAPHVKE...

AX1A_ARATH     MMITRGGAKAAKSLLVAAGPRLFSTVRTVSSHEALSASHILKPGVTSAWIWTRAP.TIGGMRFASTITLGEKTPMKEENESTGGDAAGGNN
AOX1_SOYBN                     MMMMMSRSGANRVANTAMFVAK.GLSGEVGGLRAL.YGGGVRSESTLALSEK..........EKIE.KKVGLSSAGG.N
AOX1_SAUGU     MMSSRLVGTALCRQLSHVPVPQYLPALRPTAD.TASSLLHGCSAAAPAQRAGLWPPSWFSPPRHASTLSAPAQDGGKEKAAGT....AGKVPPGEDGGAE
AOX1_MANIN                     MTVMRGLLNGGRYGNRYIWTAISLRHPEVMEGNGLESAVMQWRRMLSNAGGAEAQVKEQKEE

                                           •            •        ••           •                         •              • ••••• •    ••• •       ••
MG             TPPTWPHHGLTEKEMVDVVPGHRKPRTLGDKFAWSLVRISRWGMDKVSSLSSEQQQINKGSPTTSIVGAKPLTEAQWLSRFIFLESIAGVPGMVAGMLRH
AOX_NEUCR      TPPAWPHHGWTEEEMTSVVPEHRKPETVGDWLAWKLVRICRWATDIATGIRPE.QQVDKHHPTTATSADKPLTEAQWLVRFIFLESIAGVPGMVAGMLRH
AF031229       TKPTYRHEDFTEAGVYRVHVTHRPPRTIGDKISCYGTLFFRKCFDLVTGYAVPDP..DKPDQYKGTRWE..MTEEKWMTRCIFLESIAGVPGSVAGFVRH
AOX_HANAN      THPLFPHPKYSDEDCEAVHFVHREPKTIGDKIADRGVKFCRASFDFVTGYKKPKDVNGMLKSWEGTRYE..MTEEKWLTRCIFLESVAGVPGMVAAFIRH
AOX_ASPNG      VETAWVHPVYTEEQMKQVAIAHRDAKNLG.....RLGCVGN.GADAEMG.HGSCDWISAPSTRQGTRGQVQNDRAEVLTRFIFLESVAGVPGMVGGMLRH

AX1A_ARATH     KGDKGIASYWGVEPNKITKEDGSEWKWN⊡FRPWETYKADITIDLKKHHVPTTFLDRIAYWTVKSLRWPTDLFFQRRYGCRAMMLETVAAVPGMVGGMLLH
AOX1_SOYBN     KEEKVIVSYWGIQPSKITKKDGTEWKWN⊡FSPWGTYKADLSIDLEKHMPPTTFLDKMAFWTVKVLRYPTDVFFQRRYGCRAMMLETVAAVPGMVGGVLLH
AOX1_SAUGU     KE..AVVSYWAVPPSKVSKEDGSEWRWT⊡FRPWETYQADLSIDLHKHVPTTILDKLALRTVKALRWPTDIFFQRRYACRAMMLETVAAVPGMVGGMLLH
AOX1_MANIN     KKDAMVSNYWGISRPKITREDGSEWPWN⊡FMPWETYRSDLSIDLKKHHVPRTFMDKFAYRTVKILRVPTDIFFQRRYGCRAMMLETVAAVPGMVGGMLLH
```

Fig. 3. An alignment of the N-terminal domains of fungal AO sequences (upper set, see Fig. 2 for sequence keys) compared with a selection of plant AO sequences (lower set, AX1A_ARATH, *Arabidopsis thaliana*; AO1_SOYBN, *Glycine max*; AO1_SAUGU, *Sauromatum guttatum*; AO1_MANIN, *Magnifera indica*). The conserved, regulatory site cysteines in the plant sequences are boxed. Conserved residue positions in the fungal sequences are marked with a dot.

all pairwise permutations of sequences in this alignment, and these identities lie between 8 and 14% around an average value of 12%. Pairwise identities between members of this lower set and the *M. grisea*-C sequence, aligned on the basis of the two conserved ExxH motifs as shown in Fig. 2, range between 9 and 16% around an average of 12%. The similarity of these numbers with those shown by the structural homologues does not mitigate against *M. grisea*-C falling into this fold family. The 4-helix bundle consists of two α-helical hairpins (formed by helices 1 and 2, and 3 and 4, respectively) packed in an anti-parallel manner connected by a variable length linker region. Since the length of this linker region best matches that of the Δ-9 desaturase, this structure was chosen as the template for the homology model (in agreement with the choice made by Andersson and Nordlund for modelling of plant AO [18]). The 22-residue insertion in the *M. grisea* sequence between helices 2 and 3 was modelled as an extension to the helical hairpin motif. The choice of which *M. grisea*-C protein residues bind the iron cofactors is clear cut

from the sequence alignment with the exception of the assignment of a single metal ligand from the EEE motif. The first glutamate was chosen since this gives the best amphipathic register in the rest of the helix, however, an appropriate register could still be maintained utilising the second or third glutamate and including appropriate π-bulges in the α-helix. Such deviations from regular α-helix are seen in the MMO and RYT proteins in this region of structure. The fact that this triple-E is completely conserved in all AO sequences determined to date suggests a structural or functional role for the entire motif. The final 53 residues in the C-terminal domain were omitted from the *M. grisea*-C model since in this region there is: (a) poor structural similarity in the templates; (b) a poor level of amino acid identity with any of the templates; (c) there are only 17–34 corresponding residues in the other full length fungal sequences and (d) this region is not strongly predicted to have secondary structure (Jpred).

The geometric quality of the final *M. grisea*-C model is similar to that of the template crystal structure as assessed
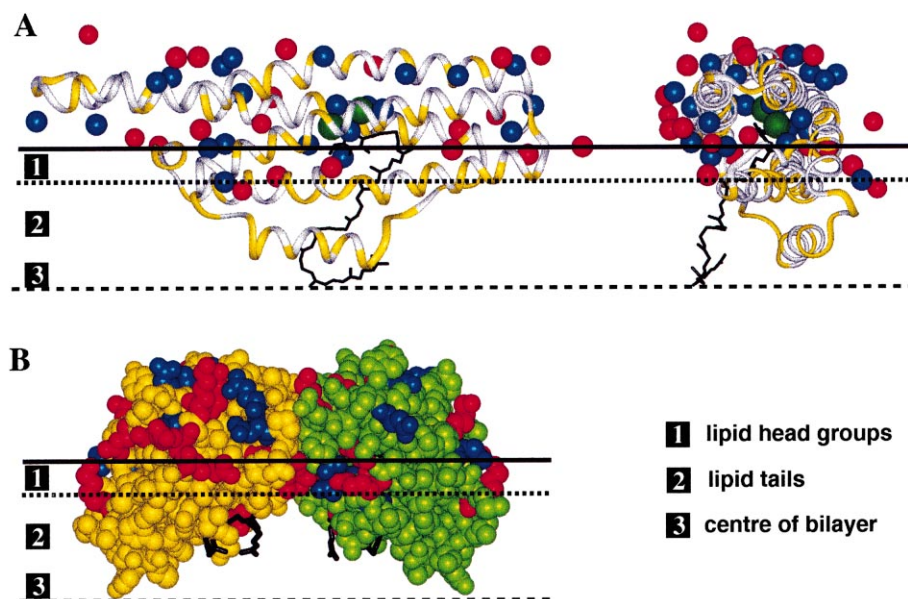

Fig. 4. The *M. grisea*-C models. A: Proposed position at a lipid bilayer/water interface, with the hydrophobic loop in the inner leaflet. The backbone of the protein is shown as a ribbon with hydrophobic residue (A, F, L, I, M, V) positions in yellow. The location of charged groups at the end of Asp, Glu, Lys and Arg residues are shown as blue (−) and red (+) spheres. Ubiquinol is represented as black sticks. Two orthogonal views of the complex are shown. B: Space filling representation of the dimer model of *M. grisea* and its proposed position in a membrane. The view is down the axis of the helical bundles. Monomers are coloured yellow and green. All atoms of all charged residues are coloured blue (−) and red (+). Ubiquinol is shown as black sticks.
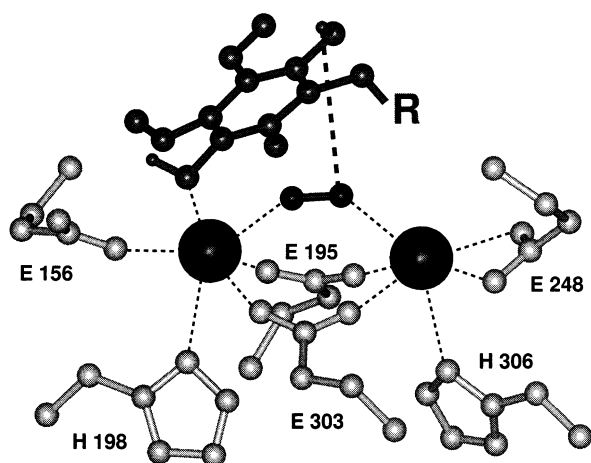
Fig. 5. The active site of the *M. grisea*-C holoenzyme model. Protein side chains coordinating the two Fe ions (large black spheres) are shown in light grey. Ubiquinol is shown in dark grey. The closest ubiquinol-OH/oxygen (O_2) distance (4.2 Å) is shown as a heavy dashed line. R represents the rest of the ubiquinol terpenoid side chain.

with Procheck. Inspection of the model shows that the 4-helix bundle has an appropriate hydrophobic core with no buried charged residues, with the exception of the iron binding ligands. The surface of the protein is liberally decorated with charged and polar residues, with the exception of the linker region between helices 2 and 3. This is a hydrophobic stretch of some 20 residues which may provide the means to associate the protein with the mitochondrial membrane (see Fig. 4A), as suggested for the equivalent region in the plant AO model of Andersson and Nordlund [18].

3.2.4. M. grisea-C ubiquinone complex. Recent studies of MMO and model compounds [25] indicate that the first reaction of the reduced di-iron centre of the protein is the formation of a μ-1,2 peroxo species where the oxygen molecule bridges the two Fe ions. This species has been modelled into the *M. grisea*-C di-iron centre and ubiquinol docked into the active site cavity. Energy minimisation yields a complex where the quinol hydrogens are poised over the iron-bound oxygen molecule for reduction to proceed (Fig. 5). Hence, the modelling process demonstrates the feasibility of generating intermediates likely to be involved in the redox reaction catalysed by fungal AO.

3.2.5. Dimer model. The interface formed by the antiparallel packing of helix-3 at the dimer interface buries a relatively small surface area, some 10% of each monomer (Fig. 4B). However, the disposition of charged residues in this region could lead to the formation of a large number of salt bridges between the monomers. Inspection shows that charged residues present could make around 16 inter-monomer salt bridges, seven of which are formed during energy minimisation.

4. Discussion

The failure of pyruvate to influence alternative respiration in *T. acuformis* mitochondria suggests that an absence of pyruvate regulation is an important feature of fungal AO. Conversely, plant AO activity increases in the presence of elevated levels of pyruvate [24], a regulatory effect attributed to the

formation of a thiohemiacetal to a conserved cysteine residue (C99 in soybean *AOX3*) located close to the N-terminus of the mature protein [5]. Mutagenesis studies on soybean *AOX3* have shown that this cysteine residue also imparts a second regulatory feature for plant AO, since it is the proposed site for formation of the sulphydryl/disulphide linkage between the two AO monomers. The redox state of this linkage is determined, at least in part, by the redox state of the quinol: quinone pool, with increased AO activity being reported for a reduced linkage [26].

The sequence alignments of the N-terminal domains of five full length fungal AOs is shown in Fig. 3 (upper set) and compared with four plant sequences (lower set). This alignment shows that the cysteine residue associated with pyruvate activation and dimer formation, which is completely conserved in all known plant sequences, is absent from all five fungal sequences. Mutation of this residue in, for example, *Arabidopsis* AO, to serine [26], glycine or alanine [27] resulted in a constitutively active AO which was unresponsive to pyruvate. The conclusion that fungal AO lacks pyruvate regulation is in keeping with the constitutive activity of many fungal AOs [4].

When Andersson and Nordlund [18] first proposed that the C-terminal domain of plant AOs is a member of the ferritin-like fold family and suggested a set of conserved residues with an iron binding role, there were only two fungal AO sequences available for comparison. There are now AO sequences of 10 fungal species in this region, including the six presented here. They all show complete conservation of the proposed iron binding residues. We present the first model of the C-terminal domain of a fungal AO (*M. grisea*). The complete sequence in this region was built onto a Δ-9 desaturase template structure and shows that the sequence is perfectly compatible with the ferritin-like fold. Hence the sequence and modelling data presented here support the notion that AOs belong to this fold family, rather than conforming to the original model developed by Siedow et al. [17] which was, of necessity, based on a paucity of sequence data. The *M. grisea*-C model supports the idea that these proteins bind to membranes via a hydrophobic linker region between the two α-helical hairpin components of the 4-helix bundle as shown in Fig. 4A.

The model of ubiquinol bound to the oxygen complex of *M. grisea*-C (Fig. 5) shows the feasibility of forming the complexes required for the oxidation of ubiquinol by oxygen in the active site. The protein offers an active site cavity of an appropriate size, shape and character to accommodate ubiquinol. The proposed binding mode of the protein to a membrane also shows that the active site is accessible to the hydrophobic interior of the lipid bilayer where the substrate ubiquinol resides (Fig. 4).

While it has not been conclusively shown that fungal AOs are dimeric, immunoblot analysis of AO from *G. graminis* shows both monomeric and dimeric forms [4]. Our modelling shows that two monomers of *M. grisea* could pack together forming a large number of salt bridges between helix-3 and helix-3′, providing a plausible mechanism for dimer formation (Fig. 4B).

Overall, data presented in this paper indicate that phytopathogenic fungal AO differs from plant AO both in its molecular organisation and in the activity regulation of the mature protein. Absence of pyruvate regulation can be explained

from analysis of the primary amino acid sequence, which indicates an absence of the activity regulating cysteine residue. The lack of a comparable cysteine at this position may also explain the constitutive activity reported for the mature fungal AO. The molecular model of the C-terminal domain of *M. grisea* AO lends further support to the proposition that AOs in general belong to the ferritin-like fold family. A model of the μ-oxo/ubiquinol holo-enzyme is consistent with the intermediates involved in the redox chemistry catalysed by this protein.

References

[1] Joseph-Horne, T. and Hollomon, D.W. (2000) Pestic. Man. Sci. 56, 24–30.

[2] Sherald, J.L. and Sisler, H.D. (1972) Plant Cell Physiol. 13, 1039–1052.

[3] Hayashi, K., Wantanabe, M., Tanaka, T. and Uesugi, Y. (1996) J. Pestic. Sci. 21, 399–403.

[4] Joseph-Horne, T., Wood, P.M., Wood, C.K., Moore, A.L., Headrick, J. and Hollomon, D. (1998) J. Biol. Chem. 273, 11127–11133.

[5] Finnegan, P.M., Whelan, J., Millar, A.H., Zhang, Q., Smith, M.K., Wiskich, J.T. and Day, D.A. (1997) Plant Physiol. 114, 455–466.

[6] Rhoads, D.M., Umbach, A.L., Sweet, C.R., Lennon, A.M., Rauch, G.S. and Siedow, J.N. (1998) J. Biol. Chem. 273, 30750–30756.

[7] Bahr, J.T. and Bonner Jr., W.D. (1973) J. Biol. Chem. 248, 3446–3450.

[8] Lambers, H. (1982) Plant Physiol. 55, 478–485.

[9] Wagner, A.M. and Moore, A.L. (1997) Biosci. Rep. 17, 319–333.

[10] Vanderleyden, J., Peeters, C., Verachtert, H. and Bertrand, H. (1980) Biochem. J. 188, 141–144.

[11] Sakajo, S., Minagawa, N. and Yoshimoto, A. (1997) Biosci. Biotech. Biochem. 61, 396–399.

[12] Kirimura, K., Yoda, M. and Usami, S. (1999) Curr. Genet. 34, 472–477.

[13] Huh, W.-K. and Kang, S.-O. (1999) J. Bacteriol. 181, 4098–4102.

[14] Sakajo, S., Minagawa, N., Komiyama, T. and Yoshimoto, A. (1991) Biochim. Biophys. Acta 1090, 102–108.

[15] Yukioka, H., Inagaki, S., Tanaka, R., Katoh, K., Miki, N., Mizutani, A. and Masuko, M. (1998) Biochim. Biophys. Acta 1442, 161–169.

[16] Li, Q., Ritzel, R.G., McLean, L.L.T., McIntosh, L., Ko, T., Bertrand, H. and Nargang, F.E. (1996) Genetics 142, 129–140.

[17] Siedow, J.N., Umbach, A.L. and Moore, A.L. (1995) FEBS Lett. 362, 10–14.

[18] Andersson, M.E. and Nordlund, P. (1999) FEBS Lett. 449, 17–22.

[19] Tamura, H., Mizutani, A., Yukioka, H., Miki, N., Ohba, K. and Masuko, M. (1999) Pestic. Sci. 55, 681–686.

[20] Lee, S.B., Milgroom, M.G. and Taylor, J.W. (1988) Fung. Genet. Newsl. 35, 23–24.

[21] Sanger, F., Nicklen, S. and Coulson, A.R. (1977) Proc. Natl. Acad. Sci. USA 74, 5463–5467.

[22] Murzin, A.G., Brenner, S.E., Hubbard, T. and Chothia, C. (1995) J. Mol. Biol. 247, 536–540.

[23] Pandya, M.J., Sessions, R.B., Williams, P.B., Dempsey, C.E., Tatham, A.S., Shewry, P.R. and Clarke, A.R. (2000) Prot. Struct. Funct. Genet. 38, 341–349.

[24] Millar, A.H., Wiskich, J.T., Whelan, J. and Day, D.A. (1993) FEBS Lett. 329, 259–262.

[25] Valentine, A.M., Stahl, S.S. and Lippard, S.J. (1999) J. Am. Chem. Soc. 121, 3876–3877.

[26] Umbach, A.L. and Siedow, J.N. (1993) Plant Physiol. 103, 845–854.

[27] Djajanegara, I., Holtzapffel, R., Finnegan, P.M., Hoefnagel, M.H.N., Berthold, D.A., Wiskich, J.T. and Day, D.A. (1999) FEBS Lett. 454, 220–224.